Improved crystal quality of GaN film with the in-plane lattice-matched $In_{0.17}Al_{0.83}N$ interlayer grown on sapphire substrate using pulsed metal–organic chemical vapor deposition*

Li Liang(李 亮), Yang Lin-An(杨林安)†, Xue Jun-Shuai(薛军帅), Cao Rong-Tao(曹荣涛), Xu Sheng-Rui(许晟瑞), Zhang Jin-Cheng(张进成), and Hao Yue(郝 跃)

State Key Discipline Laboratory of Wide Band Gap Semiconductor Technology, School of Microelectronics, Xidian University, Xi'an 710071, *China*

(Received 11 September 2013; revised manuscript received 3 November 2013; published online 10 April 2014)

We report on an improvement in the crystal quality of GaN film with an $In_{0.17}Al_{0.83}N$ interlayer grown by pulsed metal–organic chemical vapor deposition, which is in-plane lattice-matched to GaN films. The indium composition of about 17% and the reductions of both screw and edge threading dislocations (TDs) in GaN film with the InAlN interlayer are estimated by high resolution X-ray diffraction. Transmission electron microscopy (TEM) measurements are employed to understand the mechanism of reduction in TD density. Raman and photoluminescence measurements indicate that the InAlN interlayer can improve the crystal quality of GaN film, and verify that there is no additional residual stress induced into the GaN film with InAlN interlayer. Atomic force microscopy measurement shows that the InAlN interlayer brings in a smooth surface morphology of GaN film. All the results show that the insertion of the InAlN interlayer is a convenient method to achieve excellent crystal quality in GaN epitaxy.

Keywords: $In_{0.17}Al_{0.83}N$ interlayer, GaN crystal quality, dislocation reduction, photoluminescence, Raman spectra

PACS: 71.55.Eq, 78.55.Cr, 78.30.Fs **DOI:** 10.1088/1674-1056/23/6/067103

1. Introduction

Gallium nitride (GaN)-based material has attracted considerable research attention for its large breakdown voltage, high electron mobility, and high stability of temperature and chemistry.[1,2] Despite these advantages, it is well known that GaN grown on sapphire contains a high density of threading dislocations (TDs) in the range 10^{10} cm^{-2}∼10^{11} cm^{-2} due to the large discrepancies in the lattice constant and the thermal expansion coefficient between GaN and sapphire substrate,[3,4] especially for the edge component TDs, which have been found to act as electron acceptors, becoming negatively charged and thus introducing scattering centers in electron transport of device.[5,6]

In order to reduce the TD densities throughout the GaN film, previous researches indicated that the AlN interlayer and the epitaxial-lateral-overgrowth (ELOG) technologies can be employed in GaN growth. However, there exists a large lattice-mismatch between AlN and GaN layers, leading to the generation of misfit TDs at the AlN/GaN heterointerface.[7,8] In addition, ELOG technology involves several photolithographic and etching steps in order to create a patterned template for the subsequent overgrowth process, which are cumbersome and costly to achieve.[9,10] In order to improve the crystal quality of GaN film, one should explore the novel and efficient approaches to suppressing the formation of high TDs density in GaN epitaxials. In this paper, we propose an efficient method to suppress the TD densities in GaN film by introducing an InAlN interlayer which is nearly lattice-matched to GaN film. It not only avoids the misfit TD generation at the heterointerface, but also shows convenient growth processing.

Recently, $In_xAl_{1-x}N$ has attracted more and more attention for its especial characteristics.[11–15] One of the most attractive characteristics is that it can be in-plane lattice-matched to GaN with an In composition around $x = 0.17$, which makes it a promising candidate for use in optical devices and high electron mobility transistors. Fortunately, our group has successfully employed pulsed metal–organic chemical vapor deposition (PMOCVD)[16–19] to facilitate the InAlN material-related applications.

Oh *et al.*[20] reported on the effect of the InAlN interlayer on reducing the TD density in GaN film. However, we employ an improved growth method to obtain a high crystal quality InAlN interlayer, additionally, and a low temperature grown (LT) GaN protective layer to prevent the InAlN interlayer from risking indium cluster formation and indium redistribution during the subsequent high temperature top GaN growth. Furthermore, we present a different mechanism of TD reduction. In the following, we present the effect of InAlN interlayer on the suppression of TD density and the improvement of crystal quality in GaN film by using high resolution X-ray diffraction (HRXRD), transmission electron microscopy (TEM), Raman

*Project supported by the National Natural Science Foundation of China (Grant Nos. 61076079, 61274092, and 61204006) and the Key Program of the National Natural Science Foundation of China (Grant No. 61334002).

†Corresponding author. E-mail: layang@xidian.edu.cn

© 2014 Chinese Physical Society and IOP Publishing Ltd

spectroscopy, atomic force microscopy (AFM), and photoluminescence (PL) measurements.

2. Experimental procedure

Figure 1 shows a schematic diagram of the structure of GaN film with an InAlN interlayer, which was grown on a 2-in (1 in = 2.54 cm) *c*-plane sapphire substrate by PMOCVD. Trimethylauminum (TMAl), trimethylgallium (TMGa), trimethylindium (TMIn), and ammonia (NH_3) were used as precursors of Al, Ga, In, and N, respectively. Purified hydrogen was used as the carrier gas. Prior to growth, a nitridation was performed at 1060 °C for 3 min in the NH_3 ambient after having annealed the substrate in hydrogen for 7 min at 1060 °C. The growth was initiated with a 20-nm-thick AlN nucleation layer growth at 620 °C followed by a 60-nm-thick AlN layer at 1075 °C. Subsequently, a 1.5-μm-thick nominally undoped GaN buffer was grown at 940 °C.

Then, the growth temperature was ramped down to 720 °C and the carrier gas was switched from hydrogen to nitrogen for the growth of a 13-nm-thick $In_{0.17}Al_{0.83}N$ layer. Figure 2(a) shows the growth temperature, layer structures, and carrier gas for the growth of InAlN/LT-GaN. Being different from the GaN growth using conventional continual MOCVD, PMOCVD was employed to grow the InAlN interlayer, in which process the groups III and V precursors were separately introduced into the growth chamber in an alternating sequence to enhance the surface adatom migration and to improve growth efficacy. As shown in Fig. 2(b), a unit cell includes 6-s pulses of TMAl, NH_3, and a 24-s pulse of TMIn, and an NH_3 pulse always follows the metalorganic pulses. PMOCVD enables the improvement of material composition uniformity, thus obtaining a high quality InAlN interlayer. Details of InAlN epitaxy growth have been reported in our previous publications.[16–19]

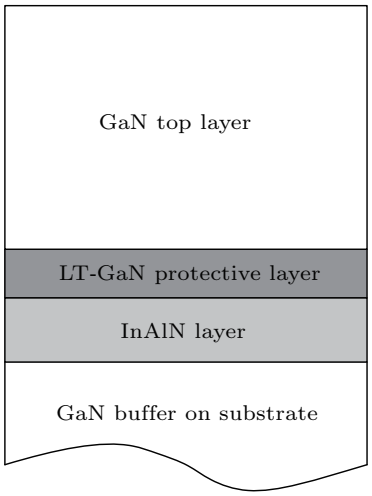


Fig. 1. Schematic diagram of GaN structure with InAlN interlayer and LT-GaN protective layer.

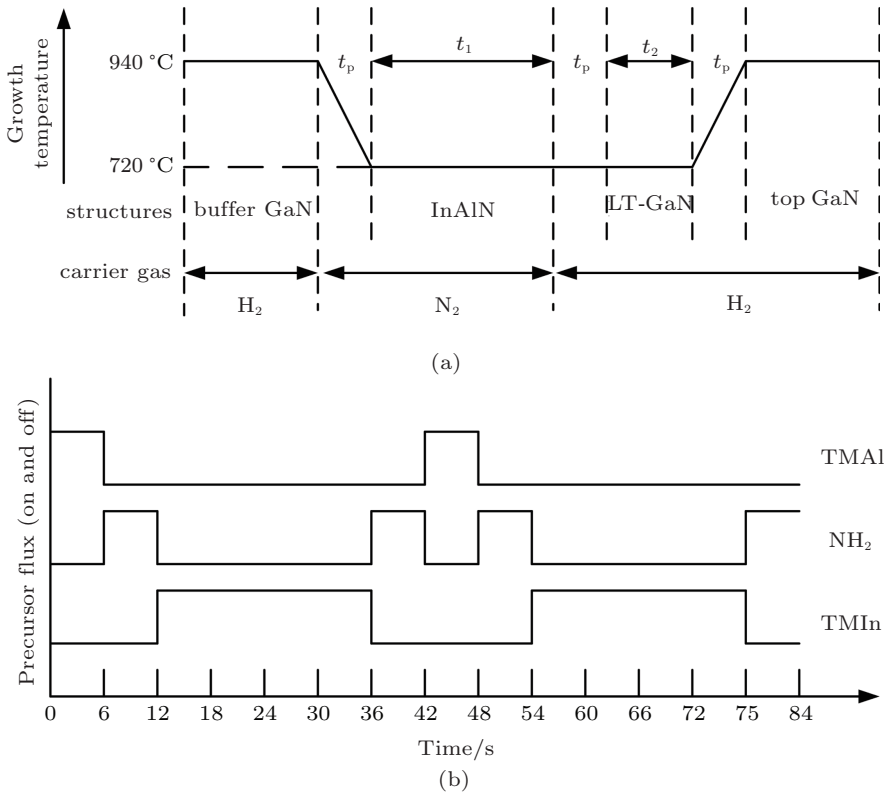


Fig. 2. (a) Schematics of the growth temperature, layer structures, and carrier gas for the growth of InAlN/LT-GaN and (b) the growth sequence of InAlN layer by PMOCVD.

It was reported that the phase separation associated with indium loss occurs during InAlN growth at high temperature.[13] To prevent the surface morphology from degrading and to avoid the risk of indium cluster formation and indium redistribution during the subsequent high temperature of the top GaN growth, a 10-nm LT-GaN protective layer was deposited on the InAlN interlayer under the same temperature (720 °C), and using hydrogen as the carrier gas. Afterward, the temperature was ramped up from 720 °C to 940 °C by t_p under hydrogen atmosphere to grow the top GaN layer. The growth times for the InAlN interlayer and LT-GaN protective layer are $t_1 = 72$ min and $t_2 = 1$ min, respectively, with the ramp up and ramp down times of $t_p = 10$ min. After that, a 1-μm-thick GaN top layer was grown at 940 °C behind the LT-GaN protective layer. In comparison, a 2.5-μm-thick GaN film without InAlN interlayer and LT-GaN protective layer was grown under the same condition. The whole layer thickness was estimated from the growth rate and confirmed by spectroscopy ellipsometry.[21]

3. Results and discussion

Figures 3(a) and 3(b) show the (0004) HRXRD ω–2θ scan for the GaN film without and with InAlN interlayer, respectively. Figure 3(a) indicates two peaks in the spectrum, the dominated peak located at about 72.9° is attributed to the GaN layer, and another peak seen at about 76.8° is attributed to the AlN nucleation layer. Besides these two peaks, figure 3(b) shows an additional InAlN peak observed at about 74.6°, therefore, the indium composition in the InAlN interlayer was estimated to be $17 \pm 1\%$ according to the reported calculation method.[22] It is noted that there is no indication of phase separation for the InAlN layer between InN and AlN peaks from HRXRD analysis. It reveals that the use of the LT-GaN protective layer makes it feasible to obtain single crystalline $In_xAl_{1-x}N$ (x∼17%) film nearly lattice-matched to GaN without phase separation.

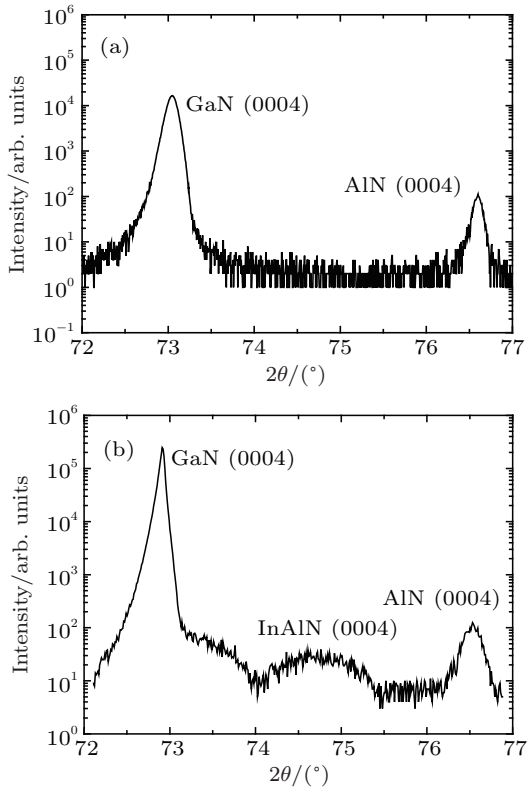


Fig. 3. HRXRD (0 0 0 4) ω–2θ scan of structures (a) without InAlN interlayer and (b) with InAlN interlayer.

In order to investigate the crystal qualities of GaN films, figures 4(a) and 4(b) show typical X-ray rocking curves of (0002) and (10$\bar{1}$2) diffractions of two GaN films, respectively. The values of full width at half maximum (FWHM) of (0002) rocking curves for GaN films without and with an InAlN interlayer are 248 arcsec and 116 arcsec, and the values of the full width at half maximum (FWHM) of (10$\bar{1}$2) rocking curve are 524 arcsec and 380 arcsec, respectively. It indicates that the insertion of InAlN interlayer can significantly improve the crystal quality of GaN film.

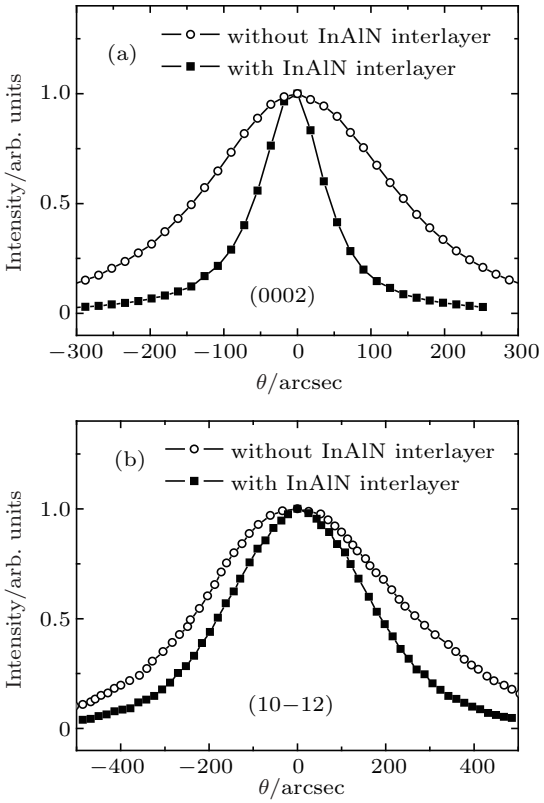
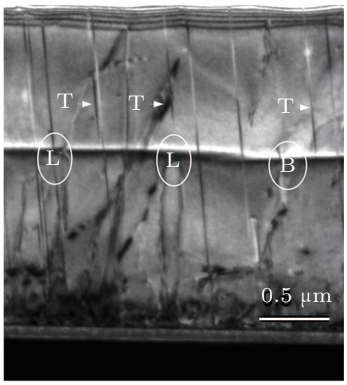


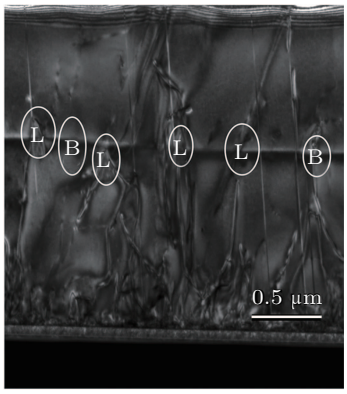
Fig. 4. Comparison of rocking curves of (a) (0002) and (b) (10$\bar{1}$2) diffractions of GaN films between without and with an InAlN interlayer.

It was reported that the densities of screw and edge component TDs for GaN films can be estimated by the FWHM of the HRXRD rocking curves on different symmetric (0002) and asymmetric (10$\bar{1}$2) planes, respectively.[23] As shown in Table 1, the calculated screw TD densities

for GaN films without and with an InAlN interlayer are 1.24×10^8 cm^{-2} and 2.70×10^7 cm^{-2}, and the edge TD densities are 1.46×10^9 cm^{-2} and 7.67×10^8 cm^{-2}, respectively, showing significant reduction of both screw and edge TD density. Insertion of interlayer in GaN film is often used to improve the film quality by reducing the TD density.[7,8,24,25] Our InAlN interlayer also appears to filter out the screw and edge component TDs. To investigate the effect of the InAlN interlayer on the TD microstructure of the GaN sample, figures 5(a) and 5(b) show TEM images of GaN film with an InAlN interlayer, where the values of diffraction vector $g = 0002$ and the $11\bar{2}0$ weak-beam cross section represent the screw-component TDs and edge-component TDs,[26] respectively. When the TDs originating from the buffer layer approach to the InAlN interlayer, some TDs are directly blocked by the InAlN interlayer, and the other TDs are forced to bend into the basal plane so as to minimize the energy.[27] Subsequently, a half loop is formed as one bended TD line encounters another one with opposite Burgers vector, resulting in the TD annihilation within the heterointerface. It is reported that the low temperature grown (LT) GaN interlayer can be considered as a TD filter.[28–32] Therefore, when the rest of the TDs thread through the heterointerface and penetrate into the LT-GaN layer, the effect of the LT-GaN layer continues to force the TDs to bend into the basal plane, and the encounter of two bended TDs lines with opposite Burgers vector brings about further TD annihilation at the heterointerface. Although there are still a few TDs generated from the surface of the InAlN layer due to the tough crystal quality of alloy expitaxy, the overall number of TDs is significantly reduced around the InAlN interlayer, bringing about the improvement in the crystal quality of the top GaN. In Figs. 5(a) and 5(b), the TD bending is marked as "B", the half loop is denoted as "L", and TD generated at the interface is referred to as "T".



(a) $g = 0002$ screw-component



(b) $g = 11\bar{2}2$ screw-component

Fig. 5. Weak-beam TEM images showing (a) the screw-component and (b) the edge-component of the TDs distribution in the GaN film with an InAlN interlayer. 'B' and 'L' correspond to bending and half-loop of TDs, and 'T' corresponds to the TDs generated at the interface.

Table 1. FWHM values of GaN (0002) and $(10\bar{1}2)$ rocking curves and corresponding TD densities for GaN films without and with an InAlN interlayer.

Structure	FWHM/arcsec		TD density/cm^{-2}	
	(0002)	$(10\bar{1}2)$	Screw	Edge
Without interlayer	248	524	1.24×10^8	1.46×10^9
With interlayer	116	380	2.70×10^7	7.67×10^8

Meanwhile, in order to verify the residual stress in GaN film induced by the InAlN interlayer, Z(XX)-Z scattering mode of the Raman spectrum was measured on GaN film. Figures 6(a) and 6(b) show the Raman spectra of GaN films without and with an InAlN interlayer measured at 300 K, respectively. In the Raman spectra, the peak located at about 418 cm^{-1} is caused by the phonon from the sapphire. Other two dominated peaks are referred to as the E_2 (high) and A_1 (LO) peaks of GaN film. Among these peaks, the E_2 (high) peak is not only sensitive to the residual stress but also associated with the quality information of GaN structure.[33,34] Figure 6(c) shows the comparison of the expanded spectrum of E_2 (high) peak between the two structures. The Raman shifts of E_2 (high) peaks of GaN films without and with the InAlN interlayer are 571.2 cm^{-1} and 571.3 cm^{-1}, respectively.

The residual stress $\sigma_{\Delta\omega}$ can be estimated by $\sigma_{\Delta\omega} = \Delta\omega/k$,[33] where $\Delta\omega$ is the measured Raman shift of the E_2 (high) peak with respect to unstressed GaN, and k is a linear stress-shift coefficient (4.5 GPa^{-1}·cm^{-1}). The compressive stresses of GaN films without and with the InAlN interlayer are estimated to be 0.489 GPa and 0.511 GPa, respectively. The discrepancy of the residual stress between two structures (0.022 GPa) is too small to need to be taken into account, which can be neglected. Therefore, we conclude that the InAlN interlayer does not introduce additional residual stress into the GaN film, which is mainly responsible for in-plane lattice match between the InAlN interlayer and the GaN film, leading to no generation of misfit TDs at the InAlN/GaN heterointerface. Additionally, the FWHM values of E_2 (high) peaks of Raman spectra can also be employed to evaluate the crystal quality. Figure 6(c) shows that FWHM values of GaN films without and with an InAlN interlayer are 5.1 cm^{-1} and 3.5 cm^{-1}, i.e., the InAlN interlayer can significantly improve the crystal quality of GaN film.

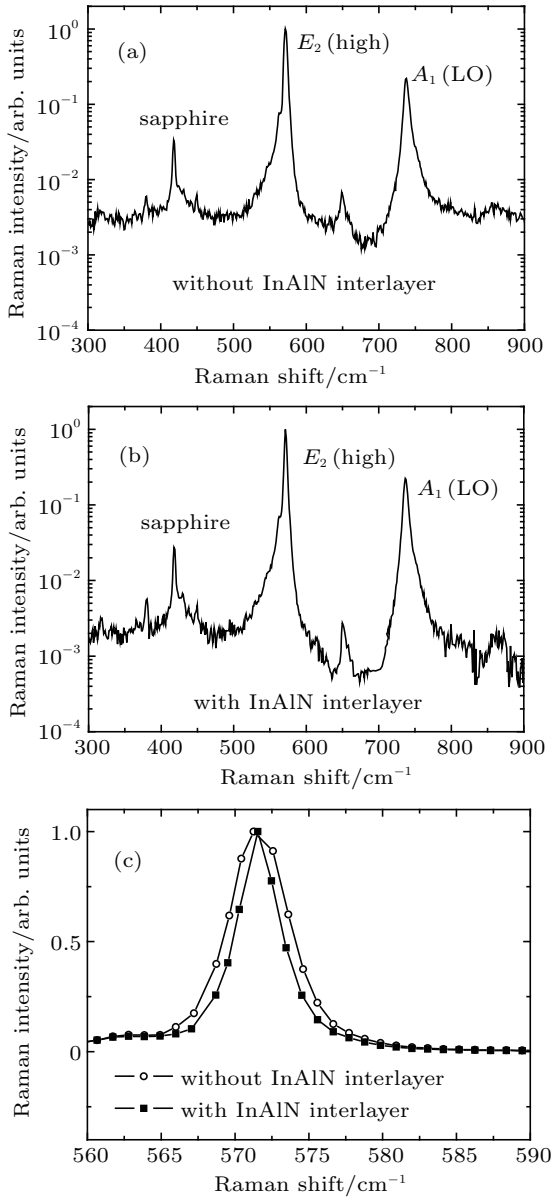


Fig. 6. Raman spectra of GaN films (a) without InAlN interlayer and (b) with InAlN interlayer, and (c) comparison between expanded spectra of the E_2 (high) peak area.

To study the effect of the InAlN interlayer on surface morphology, figures 7(a) and 7(b) show the AFM images of the top surfaces of two GaN structures, each with a scan area of 5 μm×5 μm. The root-mean-square (rms) roughness values for GaN films without and with the InAlN interlayer are 0.310 nm and 0.225 nm, respectively. Compared with the GaN film surface without InAlN interlayer, the surface with an InAlN interlayer shows highly smooth step flow patterns and less pit density associated with the TDs. Therefore, it implies that the InAlN interlayer can bring about a smoother surface morphology of epitaxial layer for GaN film.

The improvement in crystal quality for GaN film with InAlN interlayer is also evaluated by the PL spectra measured at 300 K. Figure 8(a) shows the comparison of PL spectrum between two structures without and with InAlN interlayer. As is well known, the yellow luminescence (YL) band is an important deep-level phenomenon in GaN characteristics, where the intensity ratio of YL band to band edge (BE) emission (I_{YL}/I_{BE}) corresponds to the density of the deep-acceptor point defects.[35] The I_{YL}/I_{BE} value of 0.62 for the structure without the InAlN interlayer is much higher than that of 0.34 for the structure with InAlN interlayer. It was reported that the point defects, such as gallium vacancies, can be trapped by the edge TDs,[36] which proves that there is a low density of deep-level point defects accompanied with the low density of edge TDs in GaN film with InAlN interlayer.

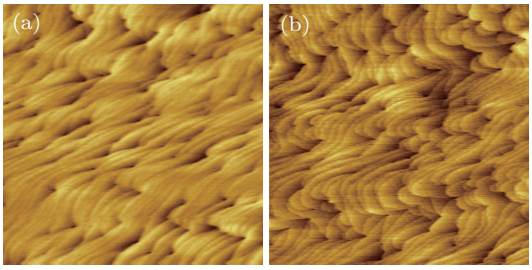


Fig. 7. (color online) AFM images of the top surface of GaN films (a) without and (b) with InAlN interlayer on a scan area of 5 μm×5 μm.

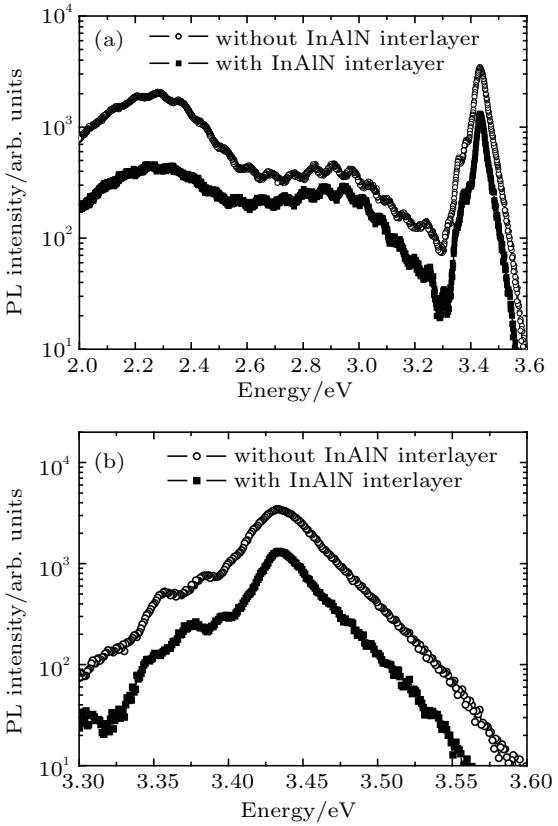


Fig. 8. Comparison of (a) PL spectrum between two GaN structures measured at 300 K, and (b) the amplified BE emission peak area.

Figure 8(b) show the expanded spectra of BE emission for two GaN films measured at 300 K, the FWHM values of BE emissions for GaN films without and with an InAlN interlayer are estimated to be 45.7 meV and 39.1 meV, respectively.

The lower value of the FWHM of BE emission means a better crystal quality, associated with the improvement of crystal quality and surface morphology in GaN film with an InAlN interlayer. In addition, the BE emission energies of GaN films without and with an InAlN interlayer are located at 3.432 eV and 3.434 eV, respectively. There is almost no shift of BE emission energy between the two structures, i.e., the InAlN interlayer does not introduce additional residual stress into the GaN film, which is consistent with the analyses of Raman results.

4. Conclusions

In this paper, we report on the improvement on the crystal quality in GaN film with an InAlN interlayer grown by PMOCVD. In order to avoid the phase separation associated with indium loss, a protective LT-GaN layer is grown at 720 °C placed behind the InAlN layer. Single crystalline $In_{0.17}Al_{0.83}N$ in GaN film is verified by HRXRD measurement. TEM measurement has demonstrated that the insertion of an InAlN interlayer in GaN film can cause the significant blocking of both screw and edge TDs. From the measurements and analyses of Raman and PL spectra, it follows that the InAlN interlayer indeed improves the crystal quality of GaN film, and introduces no additional residual stress into the GaN film. In addition, the InAlN interlayer also brings about smooth surface morphology accompanied with the reduction of TDs. Therefore, the insertion of an in-plane lattice-matched InAlN interlayer into GaN can efficiently improve crystal quality, which is of benefit to and needed for GaN epitaxy in order to obtain high power and high frequency device structures.

References

[1] Macpherson R F, Dunn G M and Pilgrim N J 2008 *Semicond. Sci. Technol.* **23** 055005

[2] Macpherson R F and Dunn G M 2008 *Appl. Phys. Lett.* **93** 062103

[3] Hacke P, Kuramata A, Domen K, Horino K and Tanahashi T 1999 *Phys. Status Solidi* **216** 639

[4] Iwaya M, Terao S, Sano T, Takanami S, Ukai T, Nakamura R, Kamiyama S, Amano H and Akasaki I 2001 *Phys. Status Solidi A* **188** 117

[5] Hansen P J, Strausser Y E, Erickson A N, Tarsa E J, Kozodoy P, Brazel E G, Ibbetson J P, Mishra U, Narayanamurti V, DenBaars S P and Speck J S 1998 *Appl. Phys. Lett.* **72** 2247

[6] Osinsky A, Gangopadhyay S, Gaska R, Williams B, Khan M A, Kuksenkov D and Temkin H 1997 *Appl. Phys. Lett.* **71** 2334

[7] Tikhonov A V, Malin T V, Zhuravlev K S, Dobos L and Pecz B 2012 *J. Cryst. Growth* **338** 30

[8] Sanchez A M, Pacheco F J, Molina S I, Stemmer J, Aderhold J and Graul J 2001 *J. Electron. Mater.* **30** 5

[9] Chakraborty A, Kim K C, Wu F, Speck J S, DenBaars S P and Mishra U K 2006 *Appl. Phys. Lett.* **89** 041903

[10] Imer B, Wu F, Speck J S and DenBaars S P 2007 *J. Cryst. Growth* **306** 330

[11] Miao Z L, Yu T J, Xu F J, Song J, Lu L, Huang C C, Yang Z J, Wang X Q, Zhang G Y, Zhang X P, Yu D P and Shen B 2010 *J. Appl. Phys.* **107** 043515

[12] Lorenz K, Franco N, Alves E, Pereira S, Watson I M, Martin R W and O'Donnell K P 2008 *J. Cryst. Growth* **310** 4058

[13] Gadanecz A, Bläsing J, Dadgar A, Hums C and Krost A 2007 *Appl. Phys. Lett.* **90** 221906

[14] Zhang J F, Wang P Y, Xue J S, Zhou Y B, Zhang J C and Hao Y 2011 *Acta Phys. Sin.* **60** 117305 (in Chinese)

[15] Wang P Y, Zhang J F, Xue J S, Zhou Y B, Zhang J C and Hao Y 2011 *Acta Phys. Sin.* **60** 117304 (in Chinese)

[16] Xue J S, Hao Y, Zhou X W, Zhang J C, Yang C K, Ou X X, Yu L S, Wang H, Yang L A and Zhang J F 2011 *J. Cryst. Growth* **314** 359

[17] Xue J S, Hao Y, Zhang J C, Zhou X W, Liu Z Y, Ma J C and Lin Z Y 2011 *Appl. Phys. Lett.* **98** 113504

[18] Xue J S, Zhang J C, Hou Y W, Zhou H, Zhang J F and Hao Y 2012 *Appl. Phys. Lett.* **100** 013507

[19] Xue J S, Zhang J C, Zhang W, Li L, Meng F N, Lu M, Ning J and Hao Y 2012 *J. Cryst. Growth* **343** 110

[20] Oh T S, Jeong H, Seo T H, Lee Y S, Park A H, Kim H, Lee K J and Suh E K 2010 *Jpn. J. Appl. Phys.* **49** 111001

[21] Miyoshi M, Egawa T and Ishikawa H 2005 *J. Vac. Sci. Technol. A* **23** 1527

[22] Angerer H, Brunner D, Freudenberg F, Ambacher O and Stutzmann M 1997 *Appl. Phys. Lett.* **71** 1504

[23] Moram M A and Vickers M E, 2009 *Rep. Prog. Phys.* **72** 036502

[24] Ren Z, Sun Q, Kwon S Y, Han J, Davitt K, Song Y K, Nurmikko A V, Cho H K, Liu W, Smart J A and Schowalter L J 2007 *Appl. Phys. Lett.* **91** 051116

[25] Sang L W, Qin Z X, Fang H, Zhou X R, Yang Z J, Shen B and Zhang G Y 2008 *Appl. Phys. Lett.* **92** 192112

[26] Ponce F A, Cherns D, Young W T and Steeds J W 1996 *Appl. Phys. Lett.* **69** 770

[27] Vilalta-Clemente A, Poisson M A, Behmenburg H, Giesen C, Heuken M and Ruterana P 2010 *Phys. Status Solidi A* **207** 1105

[28] Amano H, Iwaya M, Hayashi N, Kashima T, Katsuragawa M, Takeuchi T, Wetzel C and Akasaki I 1999 *MRS Internet J. Nitride Semicond. Res.* **4S1** G10.1.

[29] Amano H, Iwaya M, Kashima T, Katsuragawa M, Akasaki I, Han J, Hearne S, Floro J A, Chason E and Figiel J 1998 *Jpn. J. Appl. Phys.* **37** L1540

[30] Bourret-Courchesne E D, Kellermann S, Yu K M, Benamara M, Liliental-Weber Z, Washburn J, Irvine S J C and Stafford A 2000 *Appl. Phys. Lett.* **77** 3562

[31] Bourret-Courchesne E D, Yu K M, Benamara M, Liliental-Weber Z and Washburn J 2001 *J. Electron. Mater.* **30** 11

[32] Li L, Zhao D G, Jiang D S, Liu Z S, Chen P, Wu L L, Le L C, Wang H and Yang H 2013 *Chin. Phys. Lett.* **30** 028801

[33] Kisielowski C, Krüger J, Ruvimov S, Suski T, Ager J W III, Jones E, Liliental-Weber Z, Rubin M, Weber E R, Bremser M D and Davis R F 1996 *Phys. Rev. B* **54** 17745

[34] Davydov V Yu, Emtsev V V, Goncharuk I N, Smirnov A N, Petrikov V D, Mamutin V V, Vekshin V A, Ivanov S V, Smirnov M B and Inushima T 1999 *Appl. Phys. Lett.* **75** 3297

[35] Yoshikawa M, Sugie R, Murakami M, Matsunobe T, Matsuda K and Ishida H 2006 *Appl. Phys. Lett.* **88** 161905

[36] You J H and Johnson H T 1998 *Phys. Rev. B* **76** 115336